

# Radiative cooling functions for primordial molecules

C. M. Coppola,<sup>1,2\*</sup> L. Lodi<sup>1\*</sup> and J. Tennyson<sup>1\*</sup>

<sup>1</sup>Department of Physics and Astronomy, University College London, Gower Street, London WC1E 6BT

<sup>2</sup>Università degli Studi di Bari, Dipartimento di Chimica, Via Orabona 4, I-70126 Bari, Italy

Accepted 2011 March 15. Received 2011 March 15; in original form 2011 February 10

## ABSTRACT

Cooling of primordial gas plays a crucial role in the birth of the first structures in our Universe. Due to the low fractional abundance of molecular species at high redshifts, spontaneous emission rather than collisions represents the most efficient way to cool the pristine plasma. In the present work, radiative cooling functions are evaluated for the diatomic species HD, HD<sup>+</sup>, HeH<sup>+</sup>, LiH and LiH<sup>+</sup>. Cooling functions for the triatomic ions H<sub>3</sub><sup>+</sup> and H<sub>2</sub>D<sup>+</sup> are also considered. Analytic fits as functions of temperature are provided.

**Key words:** molecular processes – early Universe.

## 1 INTRODUCTION

In its present shape, our Universe appears to be a large ensemble of bound structures. These are the results of an intricate net of chemical and physical processes of increasing complexity, the first of which is fragmentation of the primordial gas clouds (see e.g. Silk 1983). One of the fundamental ingredients of this ensemble of processes is the cooling of pristine plasma. Indeed, the birth of the first objects during the evolution of the primordial gas could not have occurred without significant cooling, as the gas temperatures involved in the initial phase of the Universe are too high to allow the early clouds to gravitationally collapse. Among the plasma constituents, molecules play the most significant role as coolers of the pristine gas. Molecular cooling takes place mainly via rotational–vibrational (ro-vibrational) transitions between the internal, nuclear motion degrees of freedom. For temperatures below about 8000 K molecular cooling processes are much more efficient than the corresponding atomic ones (see e.g. Miller et al. 2010).

In models, the standard way of capturing the effects of cooling by a given species is via the *cooling function*, which gives the energy lost per second at a specified temperature. Cooling functions are made up by two main contributions. First, molecules spontaneously emit radiation while making ro-vibrational transitions; secondly, collision-induced emission can occur; this is particularly important for high-symmetry species where spontaneous emission can be very weak.

In a plasma, two key features render a molecule an efficient cooler at low temperature: its fractional abundance and its dipole moment. In the chemistry of the primordial Universe H<sub>2</sub> represents the most abundant molecular species. Its role as an efficient primordial coolant has been widely described, e.g. in the formation of the first stars (e.g. Abel, Bryan & Norman 2001) and galaxies (e.g.

Bromm et al. 2009; Benson 2010). Both collisional and radiative H<sub>2</sub> cooling contributions have been considered in the literature. The role of different collisional partners (H<sub>2</sub>, He, H<sup>+</sup> and e<sup>-</sup>) was considered by Glover & Abel (2008). Together with H<sub>2</sub>, the cooling properties of its cation H<sub>2</sub><sup>+</sup> due both to radiative and to collisional (H and e<sup>-</sup> impact excitation) pathways have been described (Suchkov & Shchekinov 1978). Both H<sub>2</sub> and H<sub>2</sub><sup>+</sup> are customarily included in molecular cooling models because of their high relative fractional abundance. However, because of their lack of a permanent dipole moment, only weak electric-quadrupole or magnetic-dipole transitions are allowed in these species, severely limiting their cooling efficiency, particularly at low density.

Considering the mole fractions of chemical species given by chemical networks such as the one by Galli & Palla (1998) (hereafter GP98), other molecular species should be added to the list of coolants. Grouping the primordial molecules as deuterated or helium-containing or lithium-enriched, HD, HD<sup>+</sup>, HeH<sup>+</sup>, LiH and LiH<sup>+</sup> represent the candidates to focus on. Their fractional abundances are expected to have the following freeze-out values ( $z \approx 10$ ):  $f(\text{HD}) \simeq 10^{-9}$ ;  $f(\text{HD}^+) \simeq 10^{-18}$ ;  $f(\text{HeH}^+) \simeq 10^{-12}$ ;  $f(\text{LiH}) \simeq 10^{-19}$ ;  $f(\text{LiH}^+) \simeq 10^{-17}$ . It is hard to form triatomic molecules at high  $z$ , but the most likely species are H<sub>3</sub><sup>+</sup> and H<sub>2</sub>D<sup>+</sup>; their fractional abundances are thought to be approximately  $f(\text{H}_3^+) \simeq 10^{-18}$  and  $f(\text{H}_2\text{D}^+) \simeq 10^{-19}$ , respectively. Collisional contributions to the cooling have been evaluated in different density regimes for HD and LiH (Lipovka, Núñez-López & Avila-Reese 2005; GP98). In particular, the effect of the most abundant collision partner H on this cooling pathway has been investigated. However, in order to complete this description, the contribution of radiative cooling has to be taken into account as well.

The present work is organized as follows. In Section 2, the equations used to compute the radiative cooling function are presented, describing the methods adopted for each molecule. Some details on previous calculations on collisional cooling functions are given. Section 3 summarizes our results and provides fits to the calculated data.

\*E-mail: carla.coppola@chimica.uniba.it (CMC); l.lodi@ucl.ac.uk (LL); j.tennyson@ucl.ac.uk (JT)

## 2 RADIATIVE COOLING FUNCTION: DEFINITION AND CALCULATIONS

The total cooling function for the chemical species  $X$  is usually approximated as (e.g. Hollenbach & McKee 1979; GP98)

$$\Lambda_X = \Lambda_{X,\text{LTE}} \left( 1 + \frac{n^{\text{cr}}}{n(\text{collider})} \right)^{-1} \quad (1)$$

where  $\Lambda_{X,\text{LTE}}$  represents the local thermodynamic equilibrium radiative contribution to the cooling function,  $n^{\text{cr}}$  and  $n(\text{collider})$  are the critical and collider density, respectively. The former is defined by

$$n^{\text{cr}} = \left( \frac{\Lambda_{X,\text{LTE}}}{\Lambda_X(n(\text{collider}))} n(\text{collider}) \right)_{n(\text{collider}) \rightarrow 0} \quad (2)$$

where  $\Lambda_X(n(\text{collider}) \rightarrow 0)$  is the low-density limit of the cooling function. Equation (1) is valid for all density regimes of the collider particle. In the high-density limit  $\Lambda_X$  reduces to  $\Lambda_{X,\text{LTE}}$ , implying that in this regime local thermal equilibrium is reached and that cooling is dominated by ro-vibrational transitions of the molecular species  $X$ .

Denoting with the letters ‘ $u$ ’ and ‘ $l$ ’ respectively the upper and lower ro-vibrational states between which a spontaneous transition may occur, the radiative cooling function is defined as

$$W(T) = \frac{1}{Z(T)} \sum_{u,l} A_{ul}(E_u - E_l)(2J_u - 1)g_u n_u, \quad (3)$$

where  $Z(T)$  represents the partition function of the molecule,  $A_{ul}$  the Einstein coefficient for the  $u \rightarrow l$  transition,  $J_u$  the rotational angular momentum of the upper rotational state,  $g_u$  the nuclear spin degeneracy (equal to 1 for all calculations below),  $E_u$  and  $E_l$  the energies of the upper and lower state and  $n_u$  the population of the upper level. As discussed above, under LTE conditions it holds

$$\begin{aligned} W(T) &\equiv \Lambda_{\text{LTE}}(T) \\ n_u &= e^{-E_u/(k_B T)} \\ Z(T) &= \sum_i (2J_i + 1) g_i e^{-E_i/(k_B T)}. \end{aligned} \quad (4)$$

Radiative cooling functions have been computed in the present work using the equations given above. As  $k_B^{-1} = 1.43878 \text{ cm K}$ , the Boltzmann factor  $n_u$  implies that at a temperature of 1000 K the cooling function is mostly determined by transitions with  $E_u \lesssim 700 \text{ cm}^{-1}$ .

Data on the emission probabilities and energy levels of the molecular species under analysis are therefore required in order to compute  $\Lambda_{\text{LTE}}$ . Depending on the available data, different strategies have been adopted for each molecular system considered. For HD and  $\text{HeH}^+$ , the relevant data have been calculated, respectively, by Abgrall et al. (1982) and Engel et al. (2005). To obtain the necessary data for the other diatomic molecules under investigation the program LEVEL 8.0 by Le Roy (2007) was used. This program solves the radial one-dimensional Schrödinger equation

$$\begin{aligned} -\frac{\hbar^2}{2\mu} \frac{d^2\Psi(r)}{dr^2} + V_J(r)\Psi(r) &= E_{v,J}\Psi(r) \\ V_J(r) &= V(r) + \frac{\hbar^2[J(J+1) - \Omega^2]}{2\mu r^2} \end{aligned} \quad (5)$$

where  $\mu$  is the reduced mass of the system,  $J$  the total rotational angular momentum,  $\Omega$  the projection of the electronic angular momentum along the internuclear axis ( $\Omega = 0$  for the states of our interest) and  $V(r)$  the diatomic potential energy curve, given as input. Once

the ro-vibrational wavefunctions  $\Psi_{v,J}$  have been obtained LEVEL can also calculate the Einstein coefficients by

$$\begin{aligned} A_{v',J' \rightarrow v'',J''} &= \left( \frac{16\pi^3}{3\varepsilon_0\hbar} \right) \frac{S(J',J'')}{2J'+1} \bar{\nu}^3 |\langle \Psi_{v',J'} | M(r) | \Psi_{v'',J''} \rangle|^2 \end{aligned} \quad (6)$$

where  $S(J',J'')$  are the Hönl–London rotational intensity factors, resulting from integration over the rotational degrees of freedom,  $\bar{\nu}$  is the wavenumber of the transition and  $M(r)$  is the diatomic dipole moment curve and is given as input. In the common case where  $\bar{\nu}$  is measured in  $\text{cm}^{-1}$  and  $M$  in Debye, the constant in brackets in equation (6) assumes the value  $3.1361891 \times 10^{-7} \text{ cm}^3 \text{ D}^{-2} \text{ s}^{-1}$ .

Calculations were carried out for the electronic ground state of the molecular systems under investigation. The following sections examine each molecule considered and give detailed information on the potential energy and dipole moment curves used to perform the calculations. Comparisons with existing data are also provided where possible.

### 2.1 HD

The role of HD in cooling phenomena of primordial plasma has been widely examined in several studies (Flower et al. 2000; Lipovka et al. 2005; Ripamonti 2007). The effect of HD cooling on the formation of massive primordial stars was analysed by Yoshida, Omukai & Hernquist (2007) and McGreer & Bryan (2008). Despite its lower fractional abundance, HD is a more efficient coolant than molecular hydrogen  $\text{H}_2$ , especially for  $T < 2000 \text{ K}$  (GP98). This is because HD molecules possess a small permanent dipole moment ( $\approx 8.3 \times 10^{-4} \text{ D}$ ; Abgrall et al. 1982) due to the asymmetry of the nuclei; by contrast, in non-deuterated molecular hydrogen only very weak quadrupole transitions are allowed.

Lipovka et al. (2005) provide a two-parameter fit of the collisional cooling function, depending on temperature and H fractional abundance. Here, we evaluate a radiative cooling function which takes into account both dipole and quadrupole electric transitions, for which we used the calculations by Abgrall et al. (1982). Results are shown in Fig. 1, and compared with the high-density limit HD cooling function fit provided by Lipovka et al. (2005), where the contribution of the lowest ro-vibrational levels up to  $v = 3$  were considered. A deviation from the high-density limit collisional

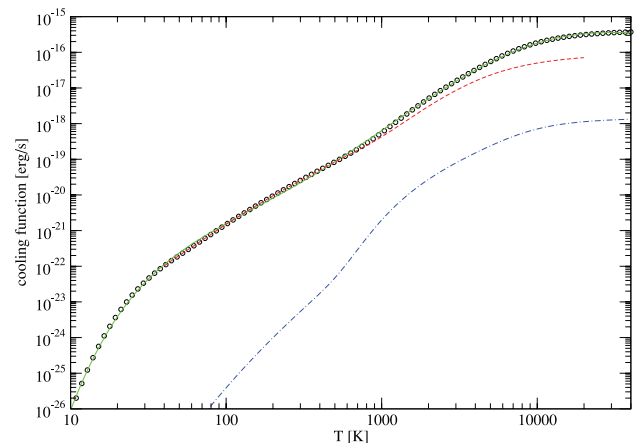


**Figure 1.** HD radiative cooling function. Circles: dipole contribution, present calculation; blue dot-dashed curve: quadrupole contribution; red dashed curve: high-density limit fit by Lipovka et al. (2005); green solid curve: fit given in Table 1.

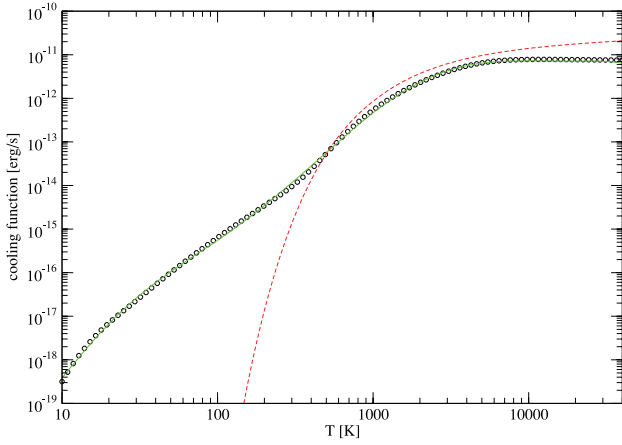


**Figure 2.**  $\text{HD}^+$  radiative cooling function: Circles: present calculation; red dashed curve: fit by Glover & Abel (2008); green solid curve: fit given in Table 1.

contribution to cooling function is found for temperatures above 700 K, where highly excited ro-vibrational states are expected to be populated.

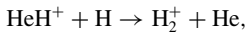
## 2.2 $\text{HD}^+$

The HD cation and its collisional contribution to the cooling during the evolution of primeval plasma have been examined by Glover & Abel (2008), where calculations were carried out assuming that there were no significant differences between the molecular ions  $\text{H}_2^+$  and  $\text{HD}^+$  in the high-density cooling limit. These authors provide an analytical expression for  $\Lambda_{\text{LTE}}$ , calculated using molecular data from Karr & Hilico (2006) on  $\text{HD}^+$  (energy levels) and Peek, Hashemi-Attar & Beckel (1979) on  $\text{H}_2^+$  (quadrupole moments).

Our calculations of the  $\text{HD}^+$  radiative cooling function were carried out using the potential energy and dipole moment curves provided by Esry & Sadeghpour (1999), in which an adiabatic reformulation of the  $\text{HD}^+$  Hamiltonian that recovers the isotopic splitting of electronic states is presented. The resulting cooling curve is shown in Fig. 2, and compared with the fit by Glover & Abel (2008). It should be noted that our calculations predict significantly increased cooling at temperatures below 100 K, where the cooling by  $\text{HD}^+$  rotational transitions is very much more efficient than the one due to its  $\text{H}_2^+$  parent ion.

## 2.3 $\text{HeH}^+$

$\text{HeH}^+$  is the first molecule formed in the initial stages of chemical synthesis in the primordial Universe chemistry (GP98; Lepp, Stancil & Dalgarno 2002; Dalgarno 2005; Hirata & Padmanabhan 2006). It represents one of the reagents for the process:



which, together with  $\text{H}+\text{H}^+$  radiative association, is the main formation pathway for the molecular hydrogen cation. The equilibrium, permanent dipole moment of  $\text{HeH}^+$ , is approximately equal to 1.66 D (Pavanello et al. 2005). Engel et al. (2005) computed line lists for different  $\text{HeH}^+$  isotopologues ( $^3\text{HeH}^+$ ,  $^4\text{HeH}^+$ ,  $^3\text{HeD}^+$ ,  $^4\text{HeD}^+$ ), and data are available electronically<sup>1</sup> both for ro-vibrational lev-

<sup>1</sup> Exomol – Molecular Line lists for Exoplanet Atmospheres, www.exomol.com (Christian Hill, Jonathan Tennyson)

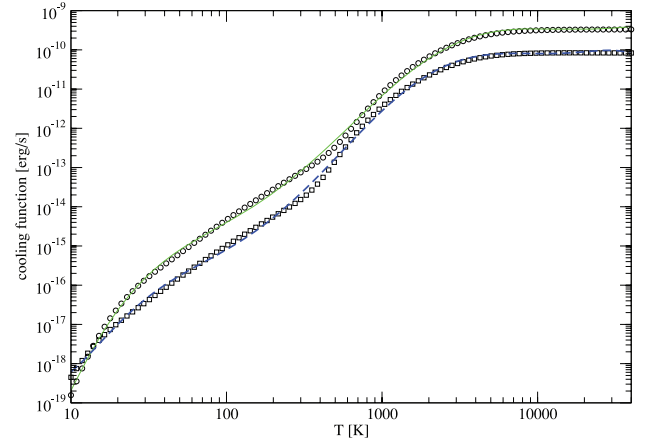


**Figure 3.**  $\text{HeH}^+$  radiative cooling function contributions. Circles:  $^3\text{HeH}^+$ ; squares:  $^3\text{HeD}^+$ ; green solid curve:  $^3\text{HeH}^+$  fit (Table 1); blue dashed curve:  $^3\text{HeD}^+$  fit (Table 1).

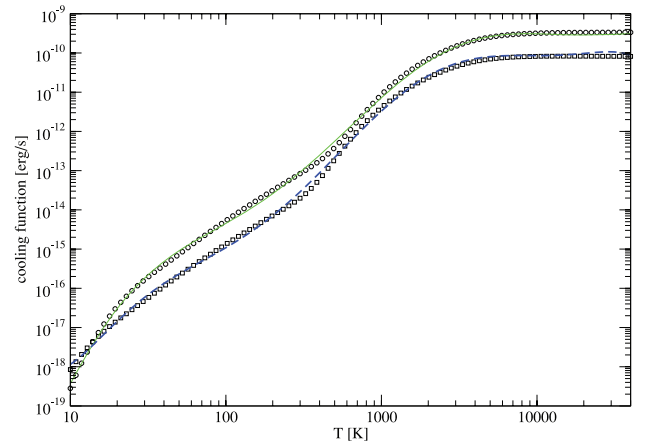


**Figure 4.**  $\text{HeH}^+$  radiative cooling function contributions. Circles:  $^4\text{HeH}^+$ ; squares:  $^4\text{HeD}^+$ ; green solid curve:  $^4\text{HeH}^+$  fit (Table 1); blue dashed curve:  $^4\text{HeD}^+$  fit (Table 1).

els and for Einstein coefficients. The cooling functions for all the isotopologues are shown in Figs 3 and 4.

## 2.4 LiH

LiH represents the primordial molecule with the largest permanent equilibrium dipole moment ( $\approx 5.88$  D; Hertzberg 1978). Several studies have modelled in detail lithium kinetics in the primordial Universe chemistry (e.g. Bougleux & Galli 1997; Lepp et al. 2002), also explicitly evaluating the cooling properties of lithium hydride due to collisional processes. The cooling properties have been described by GP98, where a fit of the collisional cooling function in the low density limit was given.

$^7\text{LiH}$  has a singlet  $X^1\Sigma^+$  ground state with an experimental equilibrium distance  $r_e = 3.015 a_0$  and a dissociation energy  $D_e = 20\,287.7 \text{ cm}^{-1}$  (Stwalley & Zemke 1993).

In virtue of its small number of electrons LiH has been the object of many quantum mechanical studies, among which we may mention the pioneering one by Mulliken (1936) and the recent ones by Bande, Nakashima & Nakatsuji (2010), Cooper & Dickinson (2009) and Gadéa & Leininger (2006). These studies, however, do

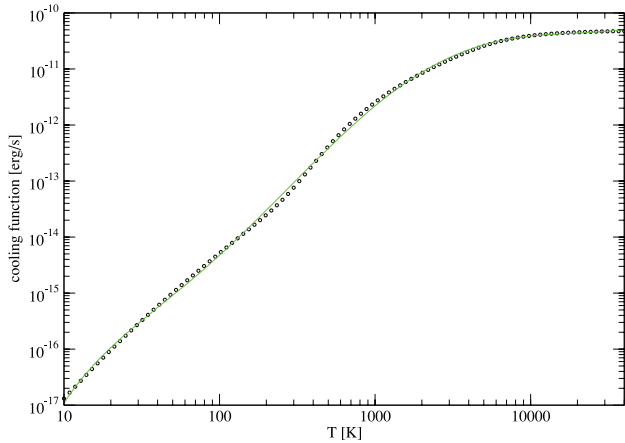


**Figure 5.** LiH radiative cooling function. Circles: present calculation; green solid curve: fit given in Table 1.

not provide in a readily usable format the potential energy curve and dipole moment curve we need to compute the cooling function. We therefore independently computed the required quantities. The computed cooling function has been plotted in Fig. 5.

#### 2.4.1 Computational detail

The potential energy and dipole moment curves have been calculated using the program MOLPRO, supplemented with the MRCC package. Descriptions of the quantum chemical methods used, along with references to the original papers, can be found, e.g., in the review by Lodi & Tennyson (2010).

The basis sets used for hydrogen belong to aug-cc-pVnZ, ( $n = T, Q, 5$ ) family by Dunning (1989). For lithium we used the recent aug-cc-pwCnZ(-DK) ( $n = T, Q, 5$ ) basis sets by Prascher et al. (2011). Basis sets with the DK suffix were especially devised to be used with the relativistic DKH Hamiltonian (see below). Computationally, it would be entirely possible to use larger basis sets but, regrettably, no larger ones are available for lithium.

The restricted Hartree–Fock (RHF) method applied to LiH wrongly dissociates to the ionic limit  $\text{Li}^+(1s^2)+\text{H}^-(1s^2)$  instead of the correct neutral pathway  $\text{Li}(1s^22s^1)+\text{H}(1s^1)$ . This behaviour is a direct consequence of the RHF model, which upon dissociation restricts molecular fragments to be spin-singlets (see e.g. Lodi & Tennyson 2010). Because the dissociation limit is wrong, methods such as CCSD(T) which rely on the RHF solution being a good approximation to the exact wavefunction may be expected to experience problems at long bond lengths. In fact, the CCSD(T) module in MOLPRO does not converge for  $r$  greater than about  $6 a_0$  (using the default settings). This may be slightly surprising because, as LiH has only 2 valence electron, method such as CCSD(T) are formally equivalent to full configuration interaction (FCI) in the valence space and should therefore be quite accurate. It is the non-linearity of the equations to be solved, together with the poor starting guess, that results in these numerical problems.

We calculated for six geometries all-electron FCI reference energies in the aug-cc-pwCQZ basis sets using the CCSDTQ code of MRCC. Computation of each FCI point involves about  $36 \times 10^6$  configuration state functions and took between 30 h and 50 h on a four-core Intel Xeon 5160 workstation with 16 GiB of memory. We compared these FCI values with several single-reference and multi-reference methods; the results of the comparisons, not discussed here, indicate that a very good balance of speed and accuracy is provided by the

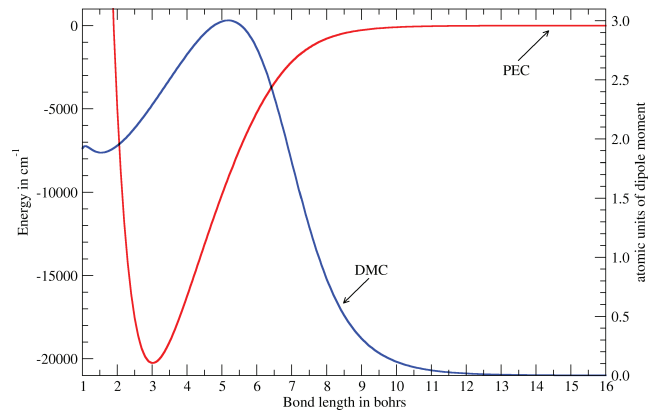


**Figure 6.** LiH potential energy curve (PEC) and dipole moment curve (DMC). The two curves use different scales for the y-axis; the left-hand side legend refers to the PEC and the right-hand side one to the DMC.

internally contracted, multi-reference averaged coupled pair functional (IC-ACPF) method based on a full-valence (two-electron, five-orbital) complete active space (eight reference configurations). This method was therefore used for further calculations. With respect to the FCI energies the IC-ACPF method predicts a dissociation energy too low by about  $6.0 \text{ cm}^{-1}$ . Computation of a IC-ACPF energy in the aug-cc-pCw5Z-DK basis set took about 4 min on the same Xeon 5160 machine.

To account for scalar-relativistic effects we considered the use of the traditional mass–velocity one-electron Darwin operator (mvd1) or, alternatively, of the fourth-order Dirac–Kroll–Hess Hamiltonian (DKH4). Relative energies computed by the two methods agree to better than  $\pm 0.05 \text{ cm}^{-1}$ . We chose the DKH4 approach. Relativistic corrections are small, affecting relative energies only by  $\pm 2 \text{ cm}^{-1}$ . The contribution of relativistic corrections to the dissociation energy is  $-0.5 \text{ cm}^{-1}$ . Finally, we remark that in our tests differences in relative energies between DK-contracted and aug-cc-pwCnZ basis sets are negligible, less than  $\pm 0.05 \text{ cm}^{-1}$  for energies up to dissociation.

The energy and dipole curves were computed for 300 uniformly spaced grid points for  $r = 1.00 a_0$  to  $r = 16.00 a_0$  with spacing  $0.05 a_0$ . The final energy values were obtained for each grid point by basis-set extrapolation of the  $n = T, Q$  and 5 values; following common practice (see e.g. Lodi & Tennyson 2010) the CAS-SCF energies were extrapolated using the functional form  $E_n = E_\infty + Ae^{-an}$  while the differences between IC-ACPF and CAS-SCF energies were extrapolated using  $E_n = E_\infty + An^3$ .

A minor complication arose because, for all basis sets employed, the CAS-SCF energies experience a discontinuity jump of about  $6 \text{ cm}^{-1}$  around  $r = 11 a_0$  if RHF orbitals are used as starting guess; as a result the IC-ACPF energies also experience a discontinuity jump of about  $1.2 \text{ cm}^{-1}$ . This problem is undoubtedly another consequence of the poor RHF starting guess; it was circumvented by starting calculations at small bond lengths and then concatenating subsequent calculations for increasing  $r$  so that the CAS-SCF orbitals from the preceding geometry were used as starting guess.

The final potential energy curve has an equilibrium bond length  $r_e = 3.014 a_0$  and a dissociation energy  $D_e = 20294 \text{ cm}^{-1}$ ; the dipole moment curve has an equilibrium dipole moment of 2.293 au, reaching a maximum of 3.003 au for  $r = 5.180 a_0$ . We may assign to  $D_e$  an uncertainty of the order of  $\pm 15 \text{ cm}^{-1}$ , mainly due to basis set incompleteness. For comparison, the non-relativistic ‘exact BO’ value quoted by Cooper & Dickinson (2009) is  $D_e = 20298.8 \text{ cm}^{-1}$ . The PEC and the DMC are plotted in Fig. 6.

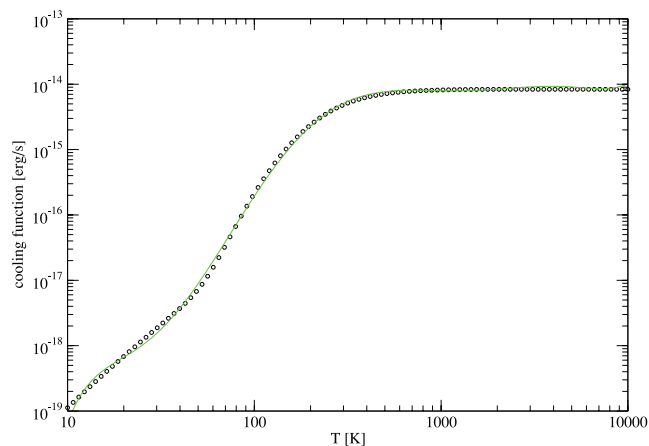


**Figure 7.**  $\text{LiH}^+$  radiative cooling function: circles: present calculation; green solid line: fit given in Table 1.

## 2.5 $\text{LiH}^+$

$\text{LiH}^+$  represents the most abundant molecular species containing lithium at low redshift. Indeed, while in the very beginning phases  $\text{LiH}$  is much more abundant than its cation, this behaviour reverses at  $z \sim 20$ , as predicted by Dalgarno & Lepp (1987) and subsequently found by kinetics models (e.g. GP98; Bogleux & Galli 1997). The reason of this behaviour is the presence of a residual ionization fraction which enhances one of the main formation channel, namely ion-atom radiative association.

So far,  $\text{LiH}^+$  has not been characterized experimentally. The present calculations, discussed below, predict a very modest dissociation energy  $D_e$  of  $1130.5 \text{ cm}^{-1}$ , an equilibrium bond length  $r_e = 4.130 a_0$  and a permanent equilibrium dipole (measured in the molecular centre-of-mass reference frame) of  $0.2773 \text{ au}$  ( $0.7048 \text{ D}$ ).

Very specialized, high-accuracy methods are applicable to  $\text{LiH}^+$  due to its small size. Very recently, Bubin, Stanke & Adamowicz (2011) presented non-adiabatic, relativistic-corrected values for the first five rotationless ( $J = 0$ ) vibrational states with a stated accuracy of better than  $0.1 \text{ cm}^{-1}$ . Among other recent studies treating  $\text{LiH}^+$  we may mention Gad ea & Leininger (2006) and Magnier (2004). However, again as in the case of  $\text{LiH}$ , because of the different focus these recent studies do not provide in a usable-format both the potential energy curve and the dipole moment curve we need to compute the cooling function. We therefore independently computed the necessary quantities. In Fig. 7 the plot of the computed cooling function is shown.

### 2.5.1 Computational details

Like the  $\text{LiH}$  case discussed in Section 2.4.1 we used the aug-cc-pwCnZ-DK ( $n = \text{T, Q, 5}$ ) basis sets and we accounted for scalar relativistic effects by specifying the DKH4 Hamiltonian. Calculations were done using MOLPRO.

The restricted open-shell Hartree-Fock method (ROHF) applied to  $\text{LiH}^+$  correctly dissociates to  $\text{Li}^+ + \text{H}$ . Single-reference methods are therefore expected to fare very well, in contrast to the  $\text{LiH}$  case discussed in Section 2.4.1.

As a preliminary test we compared using the aug-cc-pwCTZ-DK basis set 38 FCI relative energies in the range  $3.00\text{--}11.00 a_0$  with energies computed by various other methods. Here is a brief summary of the comparison, in

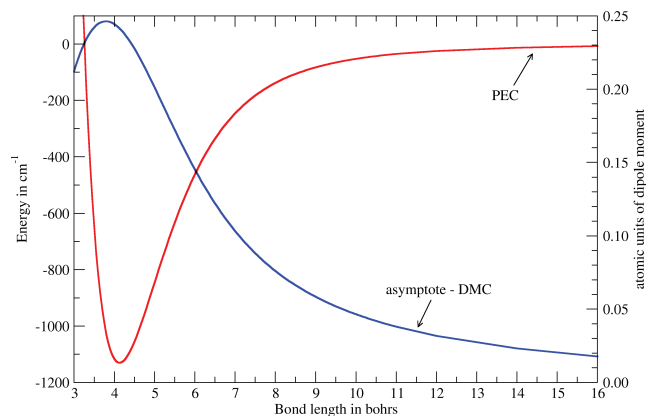


**Figure 8.**  $\text{LiH}^+$  PEC and the quantity  $0.125613r - M(r)$  (see text for details). The two curves use different scales for the y-axis; the left-hand side legend refers to the PEC, the right-hand side one to the DMC.

the form METHOD/error: ROHF/ $98.9 \text{ cm}^{-1}$ ; CISD/ $1.8 \text{ cm}^{-1}$ ; UCCSD/ $1.7 \text{ cm}^{-1}$ ; CISD+P/ $1.4 \text{ cm}^{-1}$ ; CISD+Q/ $0.6 \text{ cm}^{-1}$ ; UCCSD(T)/ $0.3 \text{ cm}^{-1}$ . The reported errors are one half of the non-parallelity error, which is defined as the difference between the maximum and the minimum of the modulus of the energy differences between two methods (Li & Paldus 1995). As expected, UCCSD(T) produces extremely accurate results; also note that this method is asymptotic to FCI upon dissociation as it is size-extensive and exact for two-electron systems. We therefore used RHF-UCCSD(T) as implemented in MOLPRO for further calculations.

Because  $\text{LiH}^+$  is a charged species the value of the dipole moment depends on the choice of the origin of the axes. As discussed by Bunker & Jensen (1998), the correct choice of the origin is the molecular centre-of-mass. MOLPRO by default does set the origin at the centre-of-mass but uses isotopically averaged nuclear masses, which is not appropriate in our case. We therefore specified the following masses:  $m(\text{Li}^+) = 7.015455 \text{ u}$  and  $m(\text{H}) = 1.0078250321 \text{ u}$ . These are atomic masses, to partially account for the electron contribution to the centre-of-mass coordinates;  $m(\text{Li}^+)$  was obtained by subtracting one electron mass to the atomic mass of Li.

With this choice of masses and taking the molecule to lie along the  $x$ -axis the coordinates of the nuclei for an inter-nuclear distance  $r$  are:  $x(\text{Li}^+) = 0.125613r$  and  $x(\text{H}) = -0.874387r$ . The dipole moment  $M(r)$  is therefore asymptotic to  $M(r) \rightarrow 0.125613r$  in this reference system.

We present in Fig. 8 a plot of the PEC and of the quantity  $0.125613r - M(r)$ , namely the difference between the asymptotic dipole and the actual one. We chose not to plot directly  $M(r)$  as, because of the asymptotic form, it would very nearly appear as a straight line.

We report here below the rotationless ( $J = 0$ ) vibrational terms  $E(v+1) - E(v)$  together with the difference with the very accurate values by Bubin et al. (2011) for  $v = 0, 1, 2, 3, 4$ :  $354.59(0.44)$ ;  $261.79(0.78)$ ;  $170.00(0.59)$ ;  $89.82(-0.07)$ ;  $35.26(0.18)$ . Our computed spectroscopic values are therefore very accurate, with errors of less than  $1 \text{ cm}^{-1}$ .

## 2.6 $\text{H}_3^+$

$\text{H}_3^+$  is one of the most interesting molecular ion in astrophysics, especially for its role in the interstellar medium chemistry. Its cooling properties have been recently considered, both in planetary

**Table 1.** Radiative cooling function fits.

Molecule		Coefficients	Molecule		Coefficients	Molecule		Coefficients
HD	$N = 5$	$a_0 = -55.5725$ $a_1 = 56.649$ $a_2 = -37.9102$ $a_3 = 12.698$ $a_4 = -2.024\ 24$ $a_5 = 0.122\ 393$	HD <sup>+</sup>	$N = 7$	$a_0 = -6.049\ 17$ $a_1 = -60.0312$ $a_2 = 98.8361$ $a_3 = -77.5575$ $a_4 = 33.4951$ $a_5 = -8.070\ 92$ $a_6 = 1.015\ 14$ $a_7 = -0.051\ 9287$	<sup>3</sup> HeH <sup>+</sup>	$N = 7$	$a_0 = -10.2807$ $a_1 = -62.9415$ $a_2 = 118.348$ $a_3 = -97.3721$ $a_4 = 42.5517$ $a_5 = -10.1946$ $a_6 = 1.263\ 35$ $a_7 = -0.063\ 3433$
<sup>4</sup> HeH <sup>+</sup>	$N = 7$	$a_0 = -7.587\ 36$ $a_1 = -68.2966$ $a_2 = 122.847$ $a_3 = -99.444$ $a_4 = 43.1409$ $a_5 = -10.3034$ $a_6 = 1.275\ 65$ $a_7 = -0.063\ 9846$	<sup>3</sup> HeD <sup>+</sup>	$N = 7$	$a_0 = 26.2717$ $a_1 = -168.493$ $a_2 = 247.288$ $a_3 = -184.299$ $a_4 = 77.0755$ $a_5 = -18.2012$ $a_6 = 2.262\ 93$ $a_7 = -0.115\ 12$	<sup>4</sup> HeD <sup>+</sup>	$N = 7$	$a_0 = 28.5384$ $a_1 = -172.458$ $a_2 = 249.811$ $a_3 = -184.786$ $a_4 = 76.9479$ $a_5 = -18.1306$ $a_6 = 2.252\ 09$ $a_7 = -0.114\ 559$
LiH	$N = 6$	$a_0 = -31.894$ $a_1 = 34.3512$ $a_2 = -31.0805$ $a_3 = 14.9459$ $a_4 = -3.723\ 18$ $a_5 = 0.455\ 555$ $a_6 = -0.021\ 6129$	LiH <sup>+</sup>	$N = 7$	$a_0 = -23.5448$ $a_1 = 9.931\ 05$ $a_2 = -8.6467$ $a_3 = 2.131\ 66$ $a_4 = 2.430\ 72$ $a_5 = -1.694\ 57$ $a_6 = 0.384\ 871$ $a_7 = -0.030\ 0114$	H <sub>2</sub> D <sup>+</sup>	$N = 6$	$a_0 = 33.8462$ $a_1 = -188.249$ $a_2 = 253.037$ $a_3 = -168.02$ $a_4 = 59.3597$ $a_5 = -10.6334$ $a_6 = 0.759\ 029$
H <sub>3</sub> <sup>+</sup>		Fit by Miller et al. (2010)						

atmosphere conditions by Miller et al. (2010) and in the primordial Universe by Glover & Savin (2009). The former work gives a fit for the radiative cooling function as a function of temperature based on the *ab initio* line list of Neale, Miller & Tennyson (1996).

## 2.7 H<sub>2</sub>D<sup>+</sup>

In the deuterium chemistry of primordial Universe, H<sub>2</sub>D<sup>+</sup> represents the most complex triatomic molecule usually introduced (Stancil, Lepp & Dalgarno 1998; Vonlanthen et al. 2009). Recently, Sochi & Tennyson (2010) have calculated a comprehensive line list of H<sub>2</sub>D<sup>+</sup> frequencies and transition probabilities. Table 1 provides an improved fit for the radiative cooling function at low temperatures, shown in Fig. 9.

## 3 CONCLUSIONS

In the present work, the cooling functions of the most abundant molecular species in the primordial Universe have been studied; calculations of the radiative contributions have been taken into account, under the hypothesis of local thermal equilibrium distributions of ro-vibrational levels. Radiative cooling functions are shown for each molecule. Analytic fits to each of these functions were obtained in the form:

$$\log_{10} W = \sum_{n=0}^N a_n (\log_{10} T)^n. \quad (7)$$

Coefficients for these fits,  $a_n$ , are provided in Table 1. The fits are valid only in the temperature range specified in the figures. Potential energy and dipole moment curves calculated in the present work,

together with the computed transition wavenumbers and Einstein coefficients, can be downloaded from [www.exomol.com](http://www.exomol.com) (Christian Hill, Jonathan Tennyson).

## ACKNOWLEDGMENTS

We thank Eveline Roueff and Herve Abgrall for making available their calculations on dipolar and quadrupolar emission probabilities of HD. CMC would also like to acknowledge Savino Longo for helpful discussion on collisional cooling functions, and MIUR and Università degli Studi di Bari, that partially supported this work (fondi di Ateneo 2010).

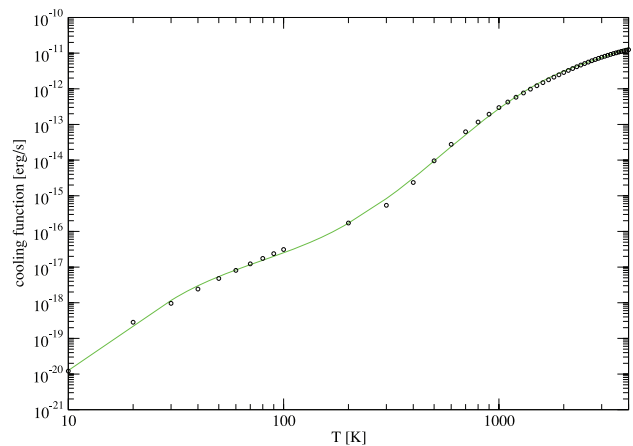


**Figure 9.** H<sub>2</sub>D<sup>+</sup> radiative cooling function. Circles: calculation by Sochi & Tennyson (2010); green solid line: fit given in Table 1.

## REFERENCES

- Abel T., Bryan G. L., Norman M. L., 2001, *Sci*, 295, 5552, 93
- Abgrall H., Roueff E., Viala Y., 1982, *A&A*, 50, 505
- Bande A., Nakashima H., Nakatsuji H., 2010, *Chem. Phys. Lett.*, 396, 347
- Benson A. J., 2010, *Phys. Rep.*, 495, 33
- Bougleux E., Galli D., 1997, *MNRAS*, 288, 638
- Bromm V., Yoshida N., Hernquist L., McKee C. F., 2009, *Nat*, 459, 49
- Bubin S., Stanke M., Adamowicz L., 2011, *J. Chem. Phys.*, 134, 024103
- Bunker P. R., Jensen P., 1998, *Molecular Symmetry and Spectroscopy*, 2nd edn. NRC Research Press, Ottawa, Ontario
- Cooper I. L., Dickinson A. S., 2009, *J. Chem. Phys.*, 131, 204303
- Dalgarno A., 2005, *J. Phys.: Conf. Ser.*, 4, 10
- Dalgarno A., Lepp S., 1987, *Proc. IAU Symp.* 120, p. 109
- Dunning T. H., 1989, *J. Chem. Phys.*, 90, 1007
- Engel E. A., Doss N., Harris G. J., Tennyson J., 2005, *MNRAS*, 357, 471
- Esry B. D., Sadeghpour H. R., 1999, *Phys. Rev. A*, 60, 3604
- Flower D. R., Le Bourlot J., Pineau des Forets G., Roueff E., 2000, *MNRAS*, 314, 753
- Gad a F. X., Leininger F. X. T., 2006, *Theor. Chem. Acc.*, 116, 566
- Galli D., Palla F., 1998, *A&A*, 335, 403 (GP98)
- Glover S. C. O., Abel T., 2008, *MNRAS*, 388, 1627
- Glover S. C. O., Savin D. W., 2009, *MNRAS*, 393, 911
- Hertzberg J., 1966, *Molecular Spectra and Molecular Structure*. Krieger Publishing Company, Malabar
- Hirata C. M., Padmanabhan N., 2006, *MNRAS*, 372, 1175
- Hollenbach D., McKee C. F., 1979, *ApJS*, 41, 555
- Karr J. Ph., Hilico L., 2006, *J. Phys. B*, 39, 2095
- Le Roy R. J., 2007, *Univ. Waterloo Chemical Physics Research Report CP-663*, see <http://scienide2.uwaterloo.ca/~rlroy/level/>
- Lepp S., Stancil P. C., Dalgarno A., 2002, *J. Phys. B.*, 35, R57.
- Li X., Paldus J., 1995, *J. Chem. Phys.*, 103, 1024
- Lipovka A., N n ez-L pez R., Avila Reese V., 2005, *MNRAS*, 361, 850
- Lodi L., Tennyson J., 2010, *J. Phys. B: At. Mol. Opt.*, 43, 133001
- Magnier S., 2004, *J. Phys. Chem. A*, 108, 1052
- McGreer I. D., Bryan G. L., 2008, *ApJ*, 685, 8
- Miller S., Stallard T., Melin H., Tennyson J., 2010, *Faraday Discuss.*, 147, 283
- MOLPRO, version 2009.1, A package of ab initio programs written by H.-J. Werner et al. (see [www.molpro.net](http://www.molpro.net))
- MRCC, a string-based quantum chemical program suite written by M. K llay [see M. K llay, P. R. Surj n, *J. Chem. Phys.* 115, 2945 (2001) as well as [www.mrcc.hu](http://www.mrcc.hu)]
- Mulliken R. S., 1936, *Phys. Rev.*, 50, 1028
- Neale L., Miller S., Tennyson J., 1996, *ApJ*, 464, 516
- Pavanello M., Bubin S., Molski M., Adamowicz L., 2005, *J. Chem. Phys.*, 123, 104306
- Peek J. M., Hashemi-Attar A.-R., Beckel C. L., 1979, *J. Chem. Phys.*, 71, 5382
- Prascher B. P., Woon D. E., Peterson K. A., Dunning T. H., Wilson A. K., 2011, *Theor. Chem. Acc.*, 128, 69
- Ripamonti E., 2007, *MNRAS*, 376, 709
- Silk J., 1983, *MNRAS*, 205, 705
- Sochi T., Tennyson J., 2010, *MNRAS*, 405, 2345
- Stancil P. C., Lepp S., Dalgarno A., 1998, *ApJ*, 509, 1, 1
- Stwalley W. C., Zemke W. T., 1993, *J. Phys. Chem. Ref. Data*, 22, 87
- Suchkov A. A., Shchekinov Yu. A., 1978, *Sov. Astron. Lett.*, 4, 164
- Vonlanthen P., Rauscher T., Winteler C., Puy D., Signore M., Dubrovich V., 2009, *A&A*, 503, 47
- Yoshida N., Omukai K., Hernquist L., 2007, *ApJ*, 667, L117

This paper has been typeset from a  $\text{\TeX}/\text{\LaTeX}$  file prepared by the author.